35th Annual Graduate Student Colloquium

Sponsored by the

Department of Geosciences

21-24 April 2003

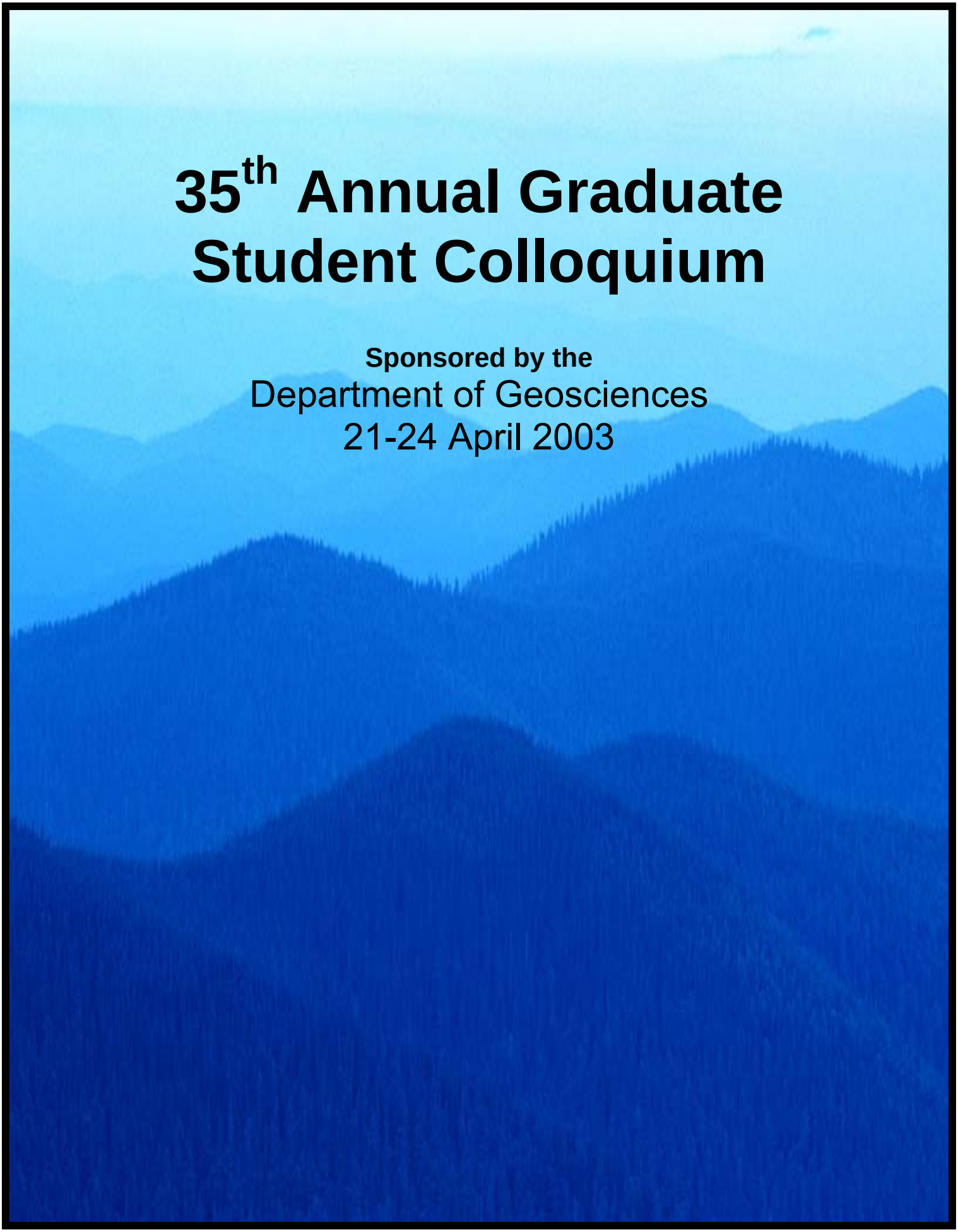

35th Annual Graduate Student Colloquium

sponsored by the
Department of Geosciences
21-24 April 2003

The Graduate Student Colloquium is a forum where students present their research or research proposal to faculty, friends, and peers. The Colloquium is hosted by the Department of Geosciences and is open to undergraduates and graduated involved in geoscience research. The format stimulates research discussion, allows students to practice for national meetings, and helps students improve speaking skills. This helps Penn State maintain and strengthen its reputation at national meetings for high quality talks, and posters with visual appeal.

Talks are a maximum of 12 minutes with an additional 3 minutes for questions. Talks will begin after Monday morning coffee, continue in a Tuesday afternoon session, and all-day Wednesday in **341 Deike**. Posters will be hung in the 3rd floor hallway of the Deike building.

The Committee wishes to thank the students for sharing their work, and the faculty for giving constructive advice. We would also like to thank the Department for financial support.

ORAL PRESENTATION SCHEDULE - MONDAY MORNING

Time	Presenter	Advisor	Title
10:30	Sara Bier	Donald Fisher	THE KAHILTNA ASSEMBLAGE: EVIDENCE FOR THE ACCRETION FO THE TALKEETNA SUPERTERRANE
10:45	Jonathan Barton	Rudy Slingerland	SELF-GENERATED SEDIMENT NOISE FROM MOVING BEDLOAD: A MODELING STUDY
11:00	Scott Miller	Rudy Slingerland	TRANSMISSION OF GEOMORPHIC SIGNALS BY LATERAL ROCKS ADVECTION: IMPLICATIONS FOR FOLD GROWTH AND SEDIMENTATION PATTERNS
11:15	Christine Gans	Kevin Furlong	CREEP, ASPERITIES AND SEISMICITY ON THE HAYWARD FAULT, CALIFORNIA
11:30	En-Chao Yeh	Donald Fisher	THE KINEMATIC ANALYSES OF THE CENTRAL RANGE, TAIWAN: A REGIONAL SCALE POP-UP STRUCTURE

ORAL PRESENTATION SCHEDULE - TUESDAY AFTERNOON

Time	Presenter	Advisor	Title
1:00	Monica Maceira	Charles Ammon	SHORT-PERIOD SURFACE-WAVE TOMOGRAPHY IN CENTRAL ASIA AND ITS APPLICATION TO SEISMIC DISCRIMINATION
1:15	Achim Herrmann	Mark Patzkowsky	OCEAN AND CLIMATE MODEL RESULTS AND THE LATE ORDOVICIAN MASS EXTINCTION
1:30	Eliana Arias	Charles Ammon	SHORT-PERIOD SURFACE WAVE TOMOGRAPHY BENEATH THE CENTRAL AND EASTERN TIBETAN PLATEAU
1:45	Matthew Bachmann	Lee Kump	MICROBIOLOGICAL NUTRIENT UPTAKE IN A TIDALLY PUMPED AQUIFER IN THE FLORIDA KEYS
2:00	Tiancong Hong	Chris Marone	NUMERICAL STUDY OF NORMAL STRESS VIBRATION ON FAULT STABILITY
2:15	Maggie Benoit	Andrew Nyblade	UPPER MANTLE SEISMIC STRUCTURE BENEATH EAST AFRICA AND THE DEPTH EXTENT OF MANTLE THERMAL ANOMALIES
2:30	Karla Panchuk	Lee Kump	BOX MODEL OF THE EPEIRIC SEA C-CYCLE

ORAL PRESENTATION SCHEDULE - WEDNESDAY MORNING

Time	Presenter	Advisor	Title
10:00	Minoo Kosarian	Charles Ammon	APPLICATION OF RECEIVER-FUNCTIONS AND SURFACE-WAVE DISPERSION ANALYSIS TO THE HOGGAR REGION, CENTRAL SAHARA, ALGERIA
10:15	Leo Peters	Sridhar Anandakrishnan	CONSTRAINING GEOLOGIC FACTOR FOR ICE STREAM FLOW IN WEST ANTARCTICA THROUGH INVERSE MODELING
10:30	David Reusch	Richard Alley	MAPPING THE WEST ANTARCTIC ATMOSPHERE WITH NEURAL NETWORKS AND ICE CORES
10:45	Matthew Spencer	Richard Alley	DEVELOPING A BUBBLE NUMBER-DENSITY PALEOCLIMATE INDICATOR FOR GLACIER ICE
11:00	Paul Winberry	Sridhar Anandakrishnan	CRUSTAL AND SEDIMENTARY STRUCTURE OF WEST ANTARCTICA

ORAL PRESENTATION SCHEDULE - WEDNESDAY AFTERNOON

Time	Presenter	Advisor	Title
1:00	Kideok Kwon	James Kubicki	THE SHORT RANGE INTERACTIONS BETWEEN A GLUCOSE AND AN OCTA-HYDROXY SILSESQUIOXANE
1:15	Beth Strickland	Peter Flemings	DEPOSITIONAL MODEL OF G-SAND AT POPEYE FIELD, GREEN CANYON 116
1:30	Eric Kuhl	Turgay Ertekin, Peter Flemings	INTEGRATION OF GEOLOGIC MODEL AND RESERVOIR SIMULATION, POPEYE FIELD, GREEN CANYON 116
1:45	Tin-Wai Lee	Peter Flemings	GASSMANN FLUID SUBSTITUTION MODELING WITH IMPLICATIONS FOR TIME-LAPSE SEISMIC ANALYSIS AT POPEYE FIELD, GREEN CANYON 116
2:00	Ben Seldon	Peter Flemings	RESERVOIR PRESSURE AND SEA FLOOR VENTING: PREDICTING TRAP INTEGRITY IN A GULF OF MEXICO DEEPWATER TURBIDITE MINIBASIN
2:15	Jane Lock	Kevin Furlong	GEOMORPHIC AND THERMAL STEADY STATE REGIMES: REALITY OR WISHFUL THINKING?

POSTER PRESENTATIONS

Presenter	Advisor	Title
Jennifer Anthony	Chris Marone	THE EFFECT OF PARTICLE CHARACTERISTICS ON STICK-SLIP INSTABILITY IN GRANULAR FAULT GOUGE
Ekaterina Bazilevskaya	Hiroshi Ohmoto	Fe-Si COMPLEXES: THEIR IMPORTANCE FOR UNDERSTANDING BANDED IRON FORMATIONS
Gavin Hayes	Kevin Furlong, Charles Ammon	CRUSTAL STRUCTURE EVOLUTION IN RESPONSE TO THE PASSAGE OF THE MENDOCINO TRIPLE JUNCTION: A RECEIVER FUNCTION ANALYSIS
Achim Hermann	Mark Patzkowsky	BIOMODULE: A JAVA PROGRAM TO HELP MODEL AND INTERPRET THE STRATIGRAPHIC RECORD
Sabrina Innocenti	Tanya Furman	EVOLUTION OF MERAPI VOLCANO, INDONESIA: A CONTRIBUTION USING CSD ANALYSIS
Minoo Kosarian	Charles Ammon	CRUSTAL STRUCTURE OF NORTH AFRICA, MIDDLE EAST AND SOUTHERN EUROPE
Christina Lopano	Peter Heaney	TIME-RESOLVED STRUCTURAL ANALYSIS OF CATION EXCHANGE REACTIONS IN BIRNESSITE USING SYNCHROTRON XRD
Yongcheol Park	Andrew Nyblade	GROUND TRUTH FROM REGIONAL SEISMIC NETWORKS IN NORTHEASTERN AFRICA
Winchelle Ian Sevilla	Charles Ammon	NEAR-REAL TIME SOURCE PARAMETER ESTIMATION OF SMALL-TO MODERATE SIZED EARTHQUAKES (Mw < 5.5) USING REGIONAL WAVEFORM DATA
Mulugeta Tuji	Andrew Nyblade	CRUSTAL STRUCTURE BENEATH THE EAST AFRICAN RIFT SYSTEM
Timothy Watson	Andrew Nyblade	A BROADBAND SEISMOLOGICAL INVESTIGATION OF THE UPPER MANTLE STRUCTURE BENEATH THE TRANS ANTARCTIC MOUNTAINS AND EAST ANTARCTIC CRATON
Aubrey Zerkle	Chris House, Lee Kump	MICROBIAL INFLUENCES ON TRACE METAL CYCLING IN A MEROMICTIC LAKE, FAYETTEVILLE GREEN LAKE, NY

ORAL PRESENTATION SCHEDULE - MONDAY MORNING

Time	Presenter	Advisor	Title
10:30	Sara Bier	Donald Fisher	THE KAHILTNA ASSEMBLAGE: EVIDENCE FOR THE ACCRETION FO THE TALKEETNA SUPERTERRANE
10:45	Jonathan Barton	Rudy Slingerland	SELF-GENERATED SEDIMENT NOISE FROM MOVING BEDLOAD: A MODELING STUDY
11:00	Scott Miller	Rudy Slingerland	TRANSMISSION OF GEOMORPHIC SIGNALS BY LATERAL ROCKS ADVECTION: IMPLICATIONS FOR FOLD GROWTH AND SEDIMENTATION PATTERNS
11:15	Christine Gans	Kevin Furlong	CREEP, ASPERITIES AND SEISMICITY ON THE HAYWARD FAULT, CALIFORNIA
11:30	En-Chao Yeh	Donald Fisher	THE KINEMATIC ANALYSES OF THE CENTRAL RANGE, TAIWAN: A REGIONAL SCALE POP-UP STRUCTURE

THE KAHILTNA ASSEMBLAGE: EVIDENCE FOR THE ACCRETION OF THE TALKEETNA SUPERTERRANE

Sara Bier
Advisor: Donald Fisher

One of them most important yet enigmatic tectonic events in south-central Alaska is the collision of the Talkeetna superterrane (the Peninsular, Alexander, and Wrangellia terranes) with the Jurassic margin of North America (the Nixon Fork and Yukon-Tanana terranes). The Kahiltna assemblage consists of the flysch that was deposited between the Talkeetna superterrane and the margin of North America, and this should preserve a record of the accretion. Regional structural investigations and dates of deformation of the Kahiltan assemblage will answer the following questions: What were the kinematics associated with superterrane accretion? What do the along-strike differences in deformation suggest about lateral variation in the geometry of the collision? What was the timing of the collision-was it synchronous or diachronous along the margin?

Along the northern margin of the Kahiltna assemblage, a mélange zone occurs as a series of exposures dismembered by ongoing strike slip faulting between the flysch of the Kahiltan terrane and the precollisional edge of the North American continent. The melange is overlain by a red and green conglomerate along a south-dipping unconformity that likely marks the base of a perched slope basin on near the toe of an accretionary wedge. Observations of melange fabrics indicate top-to-the-south shear consistent with northward directed subduction beneath North America.

Syntectonic fibers associated with cleavage formation in the Kahiltna assemblage enable incremental strain analysis to resolve the kinematics of deformation. In samples form the Peters Hills, curved antitaxial fibers indicate counterclockwise rotation of the extension direction. Given that the stretching lineation in this case is gently plunging, the strain history may provide evidence for a significant component of right-lateral shear. Samples from the Talkeetna Mountains, the Tordrillo Mountains, and north of the Denali fault also indicate right-lateral shear.

SELF-GENERATED SEDIMENT NOISE AND ITS PROPAGATION THROUGH WATER: A MODELING STUDY

Jonathan Barton
Advisor: Rudy Slingerland

Measuring the bedload sediment flux of rivers is necessary for enlightened environmental and engineering management, yet no accurate method currently exists for flood flows when the bulk of the sediment moves. We suggest that the noise made by the grains colliding with themselves and the bed might provide a measure of the flux rate. Here we explore the concept by coupling an existing model for the production of sound from the collision of two spheres with a simple sediment transport model to simulate the noise generated by moving bedload. The model allows the exploration of the relative importance of instrumentation geometry, acoustic reflection, and the mechanics of impact. The sediment transport model is stochastic, based on semi-empirical relationships for saltation length of spherical particles, rather than tracking individual particles in transport. This simplification allows the model to be run on PC in a reasonable amount of time. Results from the model show that sound produced in collisions is highly directional, producing a high-amplitude signal in the direction of impact, and a zero-amplitude signal perpendicular to that direction. The model also shows that the vertical position of the hydrophone, particularly near the bed, can have a dramatic effect on the measured signal. The results of the model qualitatively compare well with published experimental results.

TRANSMISSION OF GEOMORPHIC SIGNALS BY LATERAL ROCK ADVECTION: IMPLICATIONS FOR FOLD GROWTH AND SEDIMENTATION PATTERNS

Scott Miller
Advisor: Rudy Slingerland

Models of landscape evolution, both conceptual and numerical, have generally considered tectonics in terms of vertical rock uplift. Real bedrock velocities, however, generally include significant horizontal components. Past work has shown that the lateral advection of bedrock directly imparts a signature on steady-state topography, where rock motion is balanced by erosion. Both real and numerically simulated mountain belts exhibit asymmetrical topography, asymmetrical erosion rates, and bedrock stream long profile concavity indices that vary systematically with the direction of bedrock advection. The current study explores a further potential effect of lateral rock advection: the transmission of geomorphic information (i.e., the distribution of mass, such as topographic relief) between hydrologically unconnected drainage basins. Contrary to the common geomorphic signals that are carried down topographic gradients (e.g., water and sediment on hillslopes and in channel networks), topographic relief can be transmitted across drainage divides.

I will present preliminary result of a finite-difference landscape evolution model (CHILD) that simulates sediment transport and erosion by linear diffusion on hillslopes and a detachment-limited, unit stream power rule in streams. The model surface is structured on an irregular mesh that can readily incorporate a horizontal component to bedrock motion. In a simple simulation of a small fault-bend fold under constant tectonic forcing, both a flux steady-state and a topographic quasi-steady-state are attained which other researchers argue occur in a number of fluvial landscapes (e.g., the Siwalik Hills of the Himalayan foreland; the Santa Monica Hills of metropolitan Los Angeles; the Central Range of Taiwan). In the model landscape, drainage basins on the fold's backlimb are advected to the crest of the range and become beheaded, forming windgaps. Presented with a signal in the form of rock mass being "pushed over" the range crest, basins on the front of the structure become consequently aligned with basins on the backlimb.

Global datasets show that drainage basins typically conform to a common width-length ratio consistent with intrinsic self-similarity. If this fractal characteristic is preserved in the modeled basins, the inheritance of a new drainage basin spacing (≈ basin width) is hypothesized to cause the length of the basins to readjust (i.e., shorten or lengthen). Future tests of the model will determine if this self-similar characteristic of drainage basins is preserved. Mountain front advance or retreat, typically attributed to changes in climate or in rates or styles of tectonic activity, might also be due to drainage reorganization. Similarly, the spatial distribution of facies in foreland basins is expected to wax, wane, and /or shift if sediment sources (drainage basins) must adjust to topographic conditions on the other side of the range.

CREEP, ASPERITIES AND SEISMICITY ON THE HAYWARD FAULT, CALIFORNIA

Christine Gans
Advisor: Kevin Furlong

The Hayward Fault is documented to undergo significant creep, with some patches accommodating 50% or more of the long-term fault displacement. In spite of this, the fault has also experienced moderate to large earthquakes (most recently M ~6.8 in 1868) and is identified as a primary hazard in the San Francisco Bay region. In comparing the patterns of micro-seismicity observed on the fault with models of fault zone creep, we can investigate the partitioning among aseismic creep, creep accommodated through micro-seismicity, and strain accumulation (slip deficit), and the role that partitioning plays in the long-term deformation on the fault. To accomplish this, an analysis of the spatial distribution of moment accumulation and dissipation on the fault was undertaken. It can be shown that micro-seismicity on the Hayward fault accommodates a negligible percentage of the potential moment accumulation on the fault. Further, a new potential method for calculating the size of an asperity on a creeping fault is presented, using an independent estimator of slip. Determining asperity location and size on faults is an important component of the assessment of earthquake potential and nucleation. If one assumes that the asperity is accounting for all of the slip in the region, then using the creep models of Malservisis *et al*. [2003] to provide a value for slip, an asperity size can be determined. With accurate creep models one can hopefully better constrain a key parameter in the formula to calculate asperity size. Increasing knowledge of asperity sized, and their distribution on the fault plane, can hopefully provide insights into what an asperity might geologically represent.

THE KINEMATIC ANALYSES OF THE CENTRAL RANGE, TAIWAN: A REGIONAL SCALE POP-UP STRUCTURE

En-Chao Yeh
Advisor: Donald Fisher

Using published GPS measurements and geological data, we have investigated the current deformation rates and the regional kinematics for the Central Range, Taiwan. The new evaluations of GPS data suggest a complex pattern of deformation and three domains can be recognized with different kinematics and structure orientations. The eastern domain is characterized by shortening, minor left-lateral shear, west-dipping foliation and an along-strike lineation. The western domain is represented by shortening, significant left-lateral shear, an east-dipping foliation, and a down-dip lineation. In contrast, the central domain experiences extension as well as right- and left-lateral shear and displays a sub-vertical foliation.

The orientation of fabrics and the relative velocities and strains from GPS suggest that the Central Range is an active, regional-scale popup structure. In the western domain, ductile deformation recorded by kinematic indicators and fabrics is characterized by w-directed thrusting which is similar to the kinematics inferred from GPS surveys. In the eastern domain, the ductile deformation is consistent with early shear related to w-directed thrusting, then left-lateral shear that is overprinted by backthrusting. The difference between the ductile and brittle deformation histories in the western and eastern domains reflects the particle paths of accreted Asian crust within the mountain belt. As crust passes west to east, the rocks exhumed in the western domain have experienced an early history in the deeper parts of a w-vergent thrust belt that is overprinted by ductile left-lateral shear and the contrasting kinematics of the east-facing wedge. Consequently, the distribution of recent kinematics from GPS data and ductile kinematic patterns are consistent with the three-dimensional displacement field of a thin-skinned double-sided wedge, with the strike slip component related to oblique convergence partitioned into the interior of the mountain belt.

ORAL PRESENTATION SCHEDULE - TUESDAY AFTERNOON

Time	Presenter	Advisor	Title
1:00	Monica Maceira	Charles Ammon	SHORT-PERIOD SURFACE-WAVE TOMOGRAPHY IN CENTRAL ASIA AND ITS APPLICATION TO SEISMIC DISCRIMINATION
1:15	Achim Herrmann	Mark Patzkowsky	OCEAN AND CLIMATE MODEL RESULTS AND THE LATE ORDOVICIAN MASS EXTINCTION
1:30	Eliana Arias	Charles Ammon	SHORT-PERIOD SURFACE WAVE TOMOGRAPHY BENEATH THE CENTRAL AND EASTERN TIBETAN PLATEAU
1:45	Matthew Bachmann	Lee Kump	MICROBIOLOGICAL NUTRIENT UPTAKE IN A TIDALLY PUMPED AQUIFER IN THE FLORIDA KEYS
2:00	Tiancong Hong	Chris Marone	NUMERICAL STUDY OF NORMAL STRESS VIBRATION ON FAULT STABILITY
2:15	Maggie Benoit	Andrew Nyblade	UPPER MANTLE SEISMIC STRUCTURE BENEATH EAST AFRICA AND THE DEPTH EXTENT OF MANTLE THERMAL ANOMALIES
2:30	Karla Panchuk	Lee Kump	BOX MODEL OF THE EPEIRIC SEA C-CYCLE

SHORT-PERIOD SURFACE-WAVE TOMOGRAPHY IN CENTRAL ASIA AND ITS APPLICATION TO SEISMIC DISCRIMINATION

Monica Maceira
Advisor: Charles Ammon

The main tectonic features of central Asia are the result of the continent-continent collision between the Indian subcontinent and Eurasia. The fact that Asia is active with a significant intracontinental seismicity, together with the good broadband station coverage across most Eurasia, make surface wave tomography a powerful seismological tool to help answering question still remaining. This study focuses in the region between 70° and 95° east longitude and 35° and 50° north latitude. I analyzed broadband waveforms from 1,100 events from 1997 through May 2002 recorded at 13 seismic stations. Using multiple-filter analysis and phase-matched filter techniques, high-resolution least-squares surface wave slowness tomographic maps have been developed for the region of interest between 5 and 30 seconds. The resulting maps reveal detailed geologic and tectonic features. I carried out a resolution analysis generating 1,000 random group velocity modes, computing synthetic dispersion curves for those models, and inverting them to reproduce the tomographic maps. The variance obtained for most of the periods and most of the region is about 1%. I also validated these maps measuring new Rayleigh group velocity dispersion curves for 640 events occurred on the region of interest between January 1993 and December 1996. I analyzed group velocity residuals between map predictions and the new measurements. The overall map predictions are good . Two more tests based on the construction of phase-match filters and on the capability to detect surface waves, came out satisfactory. More over, the results of this study are being used to improve regional M_s values for the m_b-M_s earthquake-explosion discriminant.

OCEAN AND CLIMATE MODEL RESULTS AND THE LATE ORDOVICIAN MASS EXTINCTION

Achim Herrmann
Advisor: Mark Patzkowsky

Due to its association with a major glaciation and absence of evidence for extraterrestrial causes, the Late Ordovician mass extinction has generally been attributed to environmental perturbations that were the result of this glaciation. However, the nearly complete seduction of Ordovician oceanic crust limits the data set of proxies from deep ocean sea floor sediments that can be used to study the Late (Ordovician climate system. In particular we are left with mostly geochemical data from shallow epeiric seas that might not reflect the global climate characteristics. Numerical modes of Earth's atmosphere-ocean interactions therefore provide a tool to constrain those geochemical results within reasonable boundary conditions and asses the response of the climate system to different perturbations. We used numerical models to investigate the response of the Late Ordovician climate system to different perturbations. More specifically, we evaluated changes in sea level, solar insolation cycles (obliquity cycles), paleogeography and atmospheric pCO_2.

We performed sensitivity experiments using Caradocian and Ashgillian paleogeographies with the atmospheric general circulation model (AGCM) GENESIS under a range of atmospheric pCO_2 values (8-18x PAL; pre-industrial atmospheric level), high and low sea level, and two values of poleward ocean heat transport. We then couples a 3-dimensional ice sheet model to the AGCM in order to investigate the necessary boundary condition for ice sheet formation. All simulation with a high sea level and normal heat transport (i.e., modern day values) remain free off ice sheets, even with pCO_2 levels as low as 8x PAL. Assuming that pCO_2 did not fall below 8x PAL, a minimum value for this time period based on geochemical modeling and geochemical data from paleosol, a drop in pCO_2 and paleogeographic evolution coupled with an ice-albedo feedback can therefore be regard as only preconditioning factors for the Late Ordovician glaciation. In order for ice sheets to form, other factors must have changed such as a drop in sea level from its generally high Late Ordovician level and/or a reduction in poleward ocean heat transport.

We also used the ice sheet model to investigate the sensitivity of waxing and waning of these ice sheets to changes in atmospheric pCO_2 and orbital forcing at the obliquity timescale (30 to 40 k.y.). Our simulations indicate that large ice sheets, grown during extreme periods of low pCO_2 (8x PAL), can subsequently be sustained during periods of higher pCO_2 (9-10x PAL) that would otherwise prevent the growth of ice from ice-free starting conditions. Thus, if atmospheric pCO2 was one the main drivers of climate during the late Ordovician then atmospheric pCO_2 must have risen to greater than 10x PAL to melt the ice-sheets in order to end glaciation.

The AGCM results were also used to produce the forcing boundary conditions and initial conditions for an ocean general circulation model (OCGM) (MOM v.2.2) in order to investigate oceanic feedbacks. In particular, we looked at charges in ocean heat transport in response to continental drift and changes in atmospheric pCO_2 and sea level. In all simulations, a drop is sea level led to a reduction in poleward ocean heat transport. This indicates a possible positive feedback that could have to led to enhanced global cooling in response to falling sea level before or in the early stages of glaciation. Alteration in poleward ocean heat transport linked to changes of atmospheric pCO_2 also indicate that there is a threshold of 10x PAL, above which changes in poleward ocean heat transport can not be responsible for glaciation in the Late Ordovician. While continental drift can not explain the initiation of the glaciation by itself, it could explain the observed global cooling trend in the Late Ordovician through a combined poleward ocean heat transport feedback and increased ice-albedo effect if atmospheric pCO_2 was low during the entire Late Ordovician. The OGCM results indicate the due to vigorous meridional overturning, a stagnant global ocean could no have exited during the Late Ordovician, even under pCO_2 levels as high as 18x PAL when the thermal gradient between the poles and equator were relatively low. In addition, prior estimates of a sea surface temperature drop of ~11°C during the glaciation, based on oxygen isotopes, are not supported by the OGCM results. In our simulations a change of atmospheric pCO_2 from 18x PAL to 8x PAL only leads to a ~5°C drop in surface ocean temperatures.

Overall, these results help constrain environmental changes that caused the Late Ordovician mass extinction.

SHORT-PERIOD SURFACE-WAVE TOMOGRAPHY BENEATH THE CENTRAL AND EASTERN TIBETAN PLATEAU

Eliana Arias
Advisor: Charles Ammon

Despite significant effort, the mechanism driving the Tibetan Plateau uplift remains controversial because most results are from geophysical studies concentrated on t he southern part of Tibet or used data that traverses the Plateau boundary. Data from two PASSCAL experiments, the Tibetan Plateau Passive Source Seismic Experiment in 1991-1992 (TIPLT) and the INDEPTH III experiment in 1997-1999, provide and opportunity to map the subsurface geology and advance our understanding of Plateau's dynamics and tectonic evolution. We present the results of our effort to construct least-square tomographic maps of short-period Love and Rayleigh wave group velocities across the central eastern Plateau. We only utilize measurements made using station and events within the Plateau to localize sensitivity to Plateau structures. Although the short-period dispersion observations cannot reliably resolve features below the upper crust, they can be combined with other data such as global surface-wave dispersion models and receiver functions to improve resolution throughout the lithosphere.

Our inversion is based on observations using a set of 130 shallow events recorded on the 29 stations of the TIPLT, INDEPTH III, Buthan experiments and LZH station. A least-square inversion using the preliminary location and the computed new location was done for the period range of 4-50 seconds. Preliminary results for these data appear to cause noticeable scatter in the dispersion curves. The variation observed with the preliminary location is coherent with the inconsistency in small-to-moderate size event locations in global earthquake catalogs and in more refined regional locations. Currently, we are investigating the potential of an iterative tomographic and epicenter re-location procedure using surface-wave dispersion values to improve the event epicenters, and therefore to more precisely define the geological structures in the upper 20 km of the Plateau. We plan to experiment with different approaches to improve epicentral locations and to map subsurface geologic variations. Our ultimate goal is to localize short-period dispersion measurements that complement other measurements sensitive to Plateau structure such as receiver functions.

MICROBIOLOGICAL NUTRIENT UPTAKE IN A TIDALLY PUMPED AQUIFER IN THE FLORIDA KEYS

Matt Bachmann
Advisor: Lee Kump

A recent mass-balance study of a wastewater injection plume in the Florida Keys identified depleted nitrogen levels at a subsurface mud-rock interface between nitrate rich upwelling wastewaters and overlying sulfide rich anoxic confining sediments. Large vacuolated bacteria and hypothesized to utilize this chemical gradient for metabolism and growth, storing intracellularly both elemental sulfur and high concentrations of dissolved nitrate, providing a nitrogen reservoir not measured by the previous study. Sediment cores were retrieved from Florida in August 2002. A variety of microbiological techniques have been used to help identify such metabolisms in the sediment, and a finite element computer model has been used to simulate the migration of the buoyant wastewater plume. By combining microbiological tests, modeling results, and geochemical measurements, we have attempted to determine the relative importance of subsurface biota on local nutrient uptake and migration patterns in a tidally pumped confined aquifer in the Florida Keys.

NUMERICAL STUDY OF NORMAL STRESS VIBRATION ON FAULT STABILITY

Tiancong Hong
Advisor: Chris Marone

It is now well accepted that faults are not subjected to uniform stress, and these variations can be caused by temporal changes of the stress state on the faults. Temporal variation of stress may be induced by periodic changes of stress. The most pervasive periodic fluctuations of stress are due to earth tides. Direct triggering due to earth tides has been studied by Vidale *et al*. (1998) and a correlation between the rate of earthquake production at peak tidal stress and stress rate was observed. Although that correlation is not significant, Perfettini *et al.* (2001) argues that tidal triggering of earthquake still is possible.

I study the effect of periodically variable normal stress on a creeping fault stability which follow the velocity-weakening rate and state-dependent friction constitutive law for variable stress case (Linker and Dieterich, 1992). I use the spring block model incorporating radiation damping term to characterize the interaction between fault surface and crustal loading system. This numerical study indicates that a creeping fault can be destabilized and induced into stick-slip regime by a small normal stress vibration (1%). At the same time, velocity resonance phenomenon is observed.

UPPER MANTLE SEISMIC STRUCTURE BENEATH EAST AFRICA AND THE DEPTH EXTENT OF MANTLE THERMAL ANOMALIES

Margaret Benoit
Advisor: Andrew Nyblade

The origin of Cenozoic tectonism in East Africa and the Arabian Peninsula remains enigmatic. Previous studies suggest that slow seismic velocities may extend through the upper mantle beneath this region, consistent with a lower mantle origin for the Cenozoic tectonism. To further understand the origin of the tectonism in East Africa and the Arabian Peninsula, we analyze data collected from IRIS/PASSCAL broadband seismic experiments located in Saudi Arabia and Ethiopia. We employ receiver function analysis and body wave tomography to examine the upper mantle seismic velocity structure to determine the depth and lateral extent of the thermal anomaly.

Results from the northern Afar depression and the western Arabian Shield show renounced LVZs in the uppermost mantle, while the transition zone beneath these regions appears to have normal thickness. Hence, there is also little evidence to support the presence of a through-going mantle thermal anomaly beneath the northern most part of the East African rift system. Preliminary results from Ethiopia show a low velocity anomaly in the uppermost mantle located beneath the rifted region of the country.

BOX MODEL OF THE EPEIRIC SEA C-CYCLE

Karla Panchuk
Advisor: Lee Kump

Changes in the ocean C-Cycle are reflected as changes in the carbon isotope composition ($\delta^{13}C$) of carbonate sediments that form in seawater. When the $\delta^{13}C$ of marine carbonate rocks is viewed as a time series, changes in the C-cycle show up as excursions from background $\delta^{13}C$ values. For Paleozoic time, however, the marine $\delta^{13}C$ record is not derived from ocean sediments. Instead, it is derived primarily from sediments that were deposited in epeiric sea environments – that is, in shallow seas that formed on the continents. If epeiric sea carbonates were prone to the effects of local C-cycling, this makes it problematic to use the epeiric sea C-isotope record to describe the history of ocean C-cycling.

The idea of a strong local overprint on the epeiric sea C-cycle is supported by data fro the Ordovician Mohawkian Sea of Eastern Laurentia. Bulk carbonates and amorphous kerogen sampled along the 454 Ma time-slice of the Mohawkian Sea have $\delta^{13}C$ values that vary ~4.5‰ and ~7.5‰ respectively in patterns that reflect lithology, biofacies, and other geochemical data. Based on the example of the Mohawkian Sea, a box model with coupled ocean, atmosphere, and epeiric sea components was constructed to test the idea that strong patterns in epeiric sea $\delta^{13}C$ could be caused by restricted mixing of dissolved inorganic carbon (DIC) across the epeiric sea. It was found that the model cold generate ~4‰ difference between boxes representing geochemically distinct epeiric sea water masses if restricted DIC exchange were combined with differing rates of organic carbon burial in the epeiric sea boxes.

An implication of this result is that a rise or fall in sea level, which would increase or decrease the rate of DIC exchange between epeiric sea water masses is a possible cause of $\delta^{13}C$ excursions in epeiric sea carbonate sediments.

ORAL PRESENTATION SCHEDULE - WEDNESDAY MORNING

Time	Presenter	Advisor	Title
10:00	Minoo Kosarian	Charles Ammon	APPLICATION OF RECEIVER-FUNCTIONS AND SURFACE-WAVE DISPERSION ANALYSIS TO THE HOGGAR REGION, CENTRAL SAHARA, ALGERIA
10:15	Leo Peters	Sridhar Anandakrishnan	CONSTRAINING GEOLOGIC FACTOR FOR ICE STREAM FLOW IN WEST ANTARCTICA THROUGH INVERSE MODELING
10:30	David Reusch	Richard Alley	MAPPING THE WEST ANTARCTIC ATMOSPHERE WITH NEURAL NETWORKS AND ICE CORES
10:45	Matthew Spencer	Richard Alley	DEVELOPING A BUBBLE NUMBER-DENSITY PALEOCLIMATE INDICATOR FOR GLACIER ICE
11:00	Paul Winberry	Sridhar Anandakrishnan	CRUSTAL AND SEDIMENTARY STRUCTURE OF WEST ANTARCTICA

APPLICATION OF RECEIVER-FUNCTIONS AND SURFACE-WAVE DISPERSION ANALYSIS TO THE HOGGAR REGION, CENTRAL SAHARA, ALGERIA

Minoo Kosarian
Advisor: Charles Ammon

Using both joint receiver function and surface wave dispersion and H-K stacking methods we observe significant differences in the crustal thickness of the Hoggar region. These methods show the crustal thick ness and Poisson ration vary as a function of back-azimuth. The Hoggar region, located in the South Algeria, is identified as one of the most important swells on the African continent because of its complex structure. The Hoggar structure is generally interpreted as a succession of horst and grabens bound by north-south striking faults. The superposition of the Eburnean, Kibarian, and Panafrican events caused the complexity of the Hoggar. We examined data recorded by Tamanaraseet three-component broadband seismic station (TAM station) in Algeria. We computed over 150 receiver functions for each of 3 different frequency ranges in the time period 1990-2002. We obtained localized group velocities from tomographic analysis with a 2-degree resolution for both Love and Rayleigh waves in the period range from 10 to 100 seconds. The stack of receiver functions using the thickness – Vp/Vs ratio estimation procedure of Zhu and Kanamori (2000) shows roughly a 10 km variation in the depth to Moho depending on back-azimuth.

CONSTRAINING GEOLOGICAL FACTORS FOR ICE STREAM FLOW IN WEST ANTARCTICA THROUGH INVERSE MODELING

Leo Peters
Advisor: Sridhar Anandakrishnan

Two refraction seismic lines shot in the onset region of ice streams C and D in West Antarctica provide the unique opportunity of obtaining a better understanding of the subglacial geology of these ice streams. Ice streams account for a majority of the ice flow off the Antarctic continent, but the conditions that control this dynamic system are only poorly understood. I will create 2D velocity models of the two profiles using travel-time inversions of the refracted arrivals. These velocity models, along with gravity and reflection seismic data, will be used to constrain the underlying geological structure at the onset region of ice streams C and D.

Inverse modeling of the ice streams is a useful tool in determining how subglacial features influence ice stream flow and initialization. The shot-receiver geometry applied in the experiment allows for high resolution imaging of subglacial layers on the order of tens of meters in thickness. Preliminary forward modeling has revealed that the data collected thoroughly samples the upper 1-2 kilometers below the ice sheet along these two profiles. It also reveals the presence of a low-velocity zone below ice stream D (hypothesized to be a sedimentary layer), because I observe travel-time residual of up to -200 ms between the data and models without this layer. Future inverse models will focus on refining the structure along the profiles in order to minimize travel-time residuals in order to produce more accurate representation of the underlying structure. Gravity data and modeling, as well as reflection seismic data, will also be used to further constrain these models. This information can then be applied to ice velocity data in order to determine the influence subglacial geology has on ice stream flow

MAPPING THE WEST ANTARCTIC ATMOSPHERE WITH NEURAL NETWORKS AND ICE CORES

David Reusch
Advisor: Richard Alley

A deeper understanding of regional meteorology in the Antarctic is required for improved interpretations of the ever-growing body if ice-core-based paleoclimate records from this region. Artificial neural network (ANN) techniques offer new approaches to improving our record of surface observations and our understanding o the regional atmospheric circulation, two keys in this important problem.

Self-organzing maps (SOMs), and ANN-derived technique, have proved useful for analysis of synoptic-scale circulation in temperate latitudes. In short, a SOM analysis projects multidimensional data onto a two-dimension grid of generalized states. The amount of generalization is determined primarily by the dimensions of the SOM grid. (Generalization is also influenced by a number of training parameters.) The nature of SOM training leads to maximum differences between states mapping to the diagonal corners of the grid and smooth transition between states. These properties support development of synoptic climatologies with an arbitrary number of smoothly transitioning climate states, in contrast to traditional synoptic classification techniques. In this application of SOM analysis, each grid positioning the SOM map is itself a map of a meteorological parameter such as 700 mb temperature.

Results from SOM analyses are useful both for understanding the atmospheric circulation and thei ce core interpretation problem. SOM-derived maps of synoptic variables such as temperature and geopotential height can be compared to ice core data to examine the relationship between the proxy and the atmosphere. Proxy records are often viewed as surface samples for the atmosphere at local, regional and/or synoptic scales. Numerous transfer functions are often involved in this relationship. Feed-forward ANNs offer a way to relate ice core data to SOM analysis upscaling. The ANN is simply trained to predict positions in the SOM grid from corresponding ice core data. With this technique and additional ice core data, a reconstruction of the atmosphere can be developed for periods outside the span of the SOM analysis. In this work, SOM analysis is based on numerical forecast model data for 1979-1993. The upscaling ANN uses 40 year (1953-1993) ice core records of accumulation and atmospheric chemistry from four sites in central West Antarctica.

DEVELOPING A BUBBLE NUMBER-DENSITY PALEOCLIMATIC INDICATOR FOR GLACIER ICE

Matt Spencer
Advisor: Richard Alley

Grain growth in polar firn establishes a temperature- and accumulation rate-dependent bubble number density that can serve as a paleoclimatic indicator. We develop a bubble number-density model then examine the case of steady-state climate condition and find published bubble number densities yield accumulation-rate estimates, given temperature, to within ±29\% (±2σ) of accumulation-rate estimates derived from independent methods for a set of six sites in Greenland and Antarctica with mean annual temperatures ranging from 216-255 K and accumulation rates ranging from 22-500 kg m^{-2} a^{-1}.

CRUSTAL AND SEDIMENTARY STRUCTURE OF WEST ANTARCTICA

Paul Winberry
Advisor: Sridhar Anandakrishnan

Receiver function analysis is used to determine the crustal thickness and shallow sedimentary structure beneath 7 broadband stations in West Antarctica. The crustal is in general agreement with previous gravity estimates of ~30km. The main discrepancy is beneath the Bentley Subglacial trench where the crust thins to 18km, possibly representing a rift basin. The receiver function analysis also shows that much of the West Antarctic Ice Sheet is underlain by a thick layer of sediments.

ORAL PRESENTATION SCHEDULE - WEDNESDAY AFTERNOON

Time	Presenter	Advisor	Title
1:00	Kideok Kwon	James Kubicki	THE SHORT RANGE INTERACTIONS BETWEEN A GLUCOSE AND AN OCTA-HYDROXY SILSESQUIOXANE
1:15	Beth Strickland	Peter Flemings	DEPOSITIONAL MODEL OF G-SAND AT POPEYE FIELD, GREEN CANYON 116
1:30	Eric Kuhl	Turgay Ertekin, Peter Flemings	INTEGRATION OF GEOLOGIC MODEL AND RESERVOIR SIMULATION, POPEYE FIELD, GREEN CANYON 116
1:45	Tin-Wai Lee	Peter Flemings	GASSMANN FLUID SUBSTITUTION MODELING WITH IMPLICATIONS FOR TIME-LAPSE SEISMIC ANALYSIS AT POPEYE FIELD, GREEN CANYON 116
2:00	Ben Seldon	Peter Flemings	RESERVOIR PRESSURE AND SEA FLOOR VENTING: PREDICTING TRAP INTEGRITY IN A GULF OF MEXICO DEEPWATER TURBIDITE MINIBASIN
2:15	Jane Lock	Kevin Furlong	GEOMORPHIC AND THERMAL STEADY STATE REGIMES: REALITY OR WISHFUL THINKING?

THE SHORT RANGE INTERACTION BETWEEN A GLUCOSE AND AN OCTA-HYDROXY SILSESQUIOXANE

Kideok Kwon
Advisor: Jim Kubicki

Recent studies have shown that bacterial cell-surface polymers such as polysaccharides and proteins play main roles in bacterial adhesion to mineral surfaces. However, there are few studies to investigate how and how much cell-surface polymers contribute to adhesion. Most studies have been batch adsorption experiments to identify cell-polymers involvement in adhesion. Therefore, we have focused on interactions energetics between cell polymers and mineral surfaces. This research will broaden our understanding of bacterial adhesion and also possibly enable us to control adhesion.

We investigated bacterial lipopolysaccharides (LPS) first as adhesion cell-polymer. We calcuated energetics so of a glucose molecule interacting with a model silica-surface (octa-hydroxy silsesquioxane) in the short range (<1nm) using *ab initio* quantum computation. Glucose was chosen because it is the monomeric unit of the polymer Dextran, which has been used as a model LPS. Silsesquioxane was selected because it is a convenient molecule that captures the most important silanol functional groups of the silica surface.

Ab initio calculations in the gas-phase system were carried out with Gaussian 98 using both the Hartree-Fock and Density Functional Theory levels. Potential energies were calculated as a function of distance between a glucose molecule and a silsesquioxane cluster, which mimics LPS approach to silica surfaces. A force versus distance curve was predicted by derivative of the potential energy curve. The calculations predicted the formation of four H-bonds between the glucose and silsesquioxane. This interaction results in a minimum energy distance of approximately 2.4 Å between the two molecules. The total interaction energy in gas phase was -42 *kJ/mol*, which is a very weak interaction compared to interactions between water molecules and OH group of silica. Predicted interaction forces were in the range of -0.3 and 0.4 *nN*.

DEPOSTIONAL MODEL OF G-SAND AT POPEYE FIELD, GREEN CANYON 116

Beth Strickland
Advisor: Peter Flemings

The G-Sand at Popeye field (Green Canyon 116, Gulf of Mexico) is composed of two facies that were deposited with different mechanism and sediment-entry points into the basin. Gravity flows entered the basin from the north and deposited fine-grained amalgamated sheet-sands, characterized by blocky well-log signatures. Interbedded very fine-grained sands and silts that overlie the sheet facies were deposited in levee-overbank environments, by channels that bypassed the Popeye area. These bypass channels entered the basin from the north-central part of the Popeye field, and from the southwest. A late-stage channel eroded into the sheet sands and was filled with muds, and now serves as an impermeable barrier between the eastern and western reservoirs. Popeye produces gas ands condensate from late Pliocene turbidite sands compartmentalized by faults and the impermeable channel into four reservoirs at 11,500 feet depth, in 2,00 feet of water. This depositional model integrates well-log, seismic, and reservoir simulation data, and is corroborated by reservoir simulations that incorporate sand distribution maps that were interpreted based on this model.

INTEGRATION OF GEOLOGIC MODEL AND RESERVOIR SIMULATION, POPEYE FIELD, GREEN CANYON 116

Eric Kuhl
Advisor: Turgay Ertekin and Peter Flemings

A detailed geologic model forms the foundation of a reservoir simulation that demonstrates significant unique gas reserves (20 BCF) could be produced from an additional well in the northeast reservoir compartment of the Popeye field (Gulf of Mexico, GC 72/116). Popeye produces gas and condensate from late Pliocene (>1.95 Ma) turbidite sands at 11,500 ft depth in 2,000 feet of water depth. A two-layer model was developed and used in a compositional reservoir simulator; 30% porosity and 1200 mD permeability are assumed in the massive facies, and 15% porosity and 500 mD permeability are assumed in the levee/bypass facies. All faults are assumed to be impermeable. The well-matched historical production and pressure data supports the interpretation that the faults and channel are impermeable flow barriers. Simulations predict that a significant volume of hydrocarbons will not be produced by the current wells, but 20 BCP of this can be recovered with an additional well.

GASSMANN FLUID SUBSTITUTION MODELING WITH IMPLICATIONS FOR TIME-LAPSE SEISMIC ANALYSIS AT POPEYE FIELD, GREEN CANYON BLOCK 116

Christine Lee
Advisor: Peter Flemings

Gassmann fluid substitution modeling at Popeye Field predicts changes through time of the acoustic reflectivity of the G-Sand reservoir due to production-induced pressure and saturation changes. Since January 1996, the Popeye field in the Gulf of Mexico has been producing gas and condensate from the late-Pliocene turbidite G-Sand at 11,500 ft depth in 2,000 feet of water. Gassmann modeling applied to conditions after one year (1996-1997) of hydrocarbon production by two wells does not predict significant reflectivity changes. This is consistent with preliminary qualitative time-lapse analysis that shows minimal amplitude change between the pre-production and 1997 seismic surveys. Fluid substitution models of conditions after four years (1996-2000) of hydrocarbon production by four wells predict significant reduction in reflectivity. This modeled reflectivity change predicts significant amplitude reduction between the pre-production and 2000 seismic surveys. The largest change in amplitude is estimated to occur in the RM reservoir compartment, which has experienced the longest duration of production and the largest volume of recovered gas, relative to other areas of the Popeye field.

RESERVOIR PRESSURE AND SEA FLOOR VENTING: PREDICTING TRAP INTEGRITY IN A GULF OF MEXICO DEEPWATER TURBIDITE MINIBASIN

Ben Seldon
Advisor: Peter Flemings

Fluid pressures within the F-sand reservoirs in the Green Canyon 72 (GC72) field (offshore Gulf of Mexico) are controlled by venting at a sea floor expulsion feature, 13 km to the south. Given pore pressure measurements at GC72, and the assumption that the sands are permeable (fluid pressures follow the hydrostatic gradient), pore pressures at the crest of the reservoir converge on the overburden stress at the expulsion vent. At the intersection with the expulsion vent, the G-sand pressures equal 50.4 MPa (7310 psi), and the overburden stress equals 54 MPa (7825 psi). The shallower F-sand pressures are 48.1 MPa (6976 psi), which is greater than the overburden stress of 47.7 MPa (6920 psi). We interpret that overpressuring at the crest these turbidite minibasin sandstones breached the trap integrity. Fluids leaked out of this crest, resulting in shallow gas washout and seafloor expulsion above the crest. The seafloor vent is expressed as a series of conical features up to 900 meters (2953 feet) in diameter and with a relief of up to 60 meters (197 feet). The observation that sandstone pressures equal the overburden stress at expulsion vents can be used to predict the pore pressure in any reservoir that is hydraulically connected with this expulsion event. This methodology can be used to predict trap integrity in an exploration setting and to design safe and economic drilling programs within geopressured basins.

GEOMORPHIC AND THERMAL STEADY STATE REGIMES: REALITY OR WISHFUL THINKING?

Jane Lock
Advisor: Kevin Furlong

In many tectonic geomorphic studies, it is assumed that rates of uplift within an orogen are matched by rates of exhumation producing a steady-state orogen. However, the tools used to determine exhumation are thermally driven (e.g. Fission Track, U-Th/He) and exhumation can substantially perturb the crustal thermal regime. Since knowing the thermal regime is key to determining exhumation from thermochronology, problems arise. In order to interpret a rate of exhumation an assumption that an area is in thermal 'steady state' is made, which in young active orogens unlikely exists.

Taiwan, the Southern Alps, Fiordland, and Nanga Parbat are relatively young mountain belts that have begun to uplift or have experienced increased rates of uplift during the past 5-10Ma. As there is a time lag between the onset of uplift and achieving geomorphic seady sate and again between reaching geomorphic steady state and thermal steady state, these orogens may be too young to have achieved this final stage. Additionally, young orogens may not have experienced a constant rate of uplift and denudation in the time over which the thermochronometers average. Certainly, in the case of the Southern Alps, present uplift rates can not have existed since uplift begun. Therefore, an apparent age is recording a transient thermal state. Even in a case where geomorphic steady state exists i.e. exhumation balances uplift, it is unlikely that a thermal steady state has been reached. This precludes the simple interpretation of exhumation rates often made.

When multiple thermochronometers are used, inconsistencies can arise. For example, an increase in the rate of uplift is often observed when comparing the rates of exhumation using different thermochronometers. Our modeling shoes that in some cases this phenomena is actually eliminated by considering the transient nature of the thermal regime following the onset of uplift and exhumation an active orogen.

In order to accurately determine exhumation rate from a thermochronometric apparent age, feedbacks between exhumation and thermal processed need to be considered.

POSTER PRESENTATIONS

Presenter	Advisor	Title
Jennifer Anthony	Chris Marone	THE EFFECT OF PARTICLE CHARACTERISTICS ON STICK-SLIP INSTABILITY IN GRANULAR FAULT GOUGE
Ekaterina Bazilevskaya	Hiroshi Ohmoto	Fe-Si COMPLEXES: THEIR IMPORTANCE FOR UNDERSTANDING BANDED IRON FORMATIONS
Gavin Hayes	Kevin Furlong, Charles Ammon	CRUSTAL STRUCTURE EVOLUTION IN RESPONSE TO THE PASSAGE OF THE MENDOCINO TRIPLE JUNCTION: A RECEIVER FUNCTION ANALYSIS
Achim Hermann	Mark Patzkowsky	BIOMODULE: A JAVA PROGRAM TO HELP MODEL AND INTERPRET THE STRATIGRAPHIC RECORD
Sabrina Innocenti	Tanya Furman	EVOLUTION OF MERAPI VOLCANO, INDONESIA: A CONTRIBUTION USING CSD ANALYSIS
Minoo Kosarian	Charles Ammon	CRUSTAL STRUCTURE OF NORTH AFRICA, MIDDLE EAST AND SOUTHERN EUROPE
Christina Lopano	Peter Heaney	TIME-RESOLVED STRUCTURAL ANALYSIS OF CATION EXCHANGE REACTIONS IN BIRNESSITE USING SYNCHROTRON XRD
Yongcheol Park	Andrew Nyblade	GROUND TRUTH FROM REGIONAL SEISMIC NETWORKS IN NORTHEASTERN AFRICA
Winchelle Ian Sevilla	Charles Ammon	NEAR-REAL TIME SOURCE PARAMETER ESTIMATION OF SMALL-TO MODERATE SIZED EARTHQUAKES (Mw < 5.5) USING REGIONAL WAVEFORM DATA
Mulugeta Tuji	Andrew Nyblade	CRUSTAL STRUCTURE BENEATH THE EAST AFRICAN RIFT SYSTEM
Timothy Watson	Andrew Nyblade	A BROADBAND SEISMOLOGICAL INVESTIGATION OF THE UPPER MANTLE STRUCTURE BENEATH THE TRANS ANTARCTIC MOUNTAINS AND EAST ANTARCTIC CRATON
Aubrey Zerkle	Chris House, Lee Kump	MICROBIAL INFLUENCES ON TRACE METAL CYCLING IN A MEROMICTIC LAKE, FAYETTEVILLE GREEN LAKE, NY

THE EFFECT OF PARTICLE CHARACTERISTICS ON STICK-SLIP INSTABILITY IN GRANULAR FAULT GOUGE

Jennifer Anthony
Advisor: Chris Marone

The characteristics of fault gouge material affect the amount of pre-seismic slip and stress drop during stick-slip instability in the laboratory. In order to improve our understanding of pre-seismic and co-seismic earthquake instability, we performed laboratory experiments using a double-direct-shear testing apparatus. This assembly includes three rigid forcing blocks with two gouge layers sandwiched between rough surfaces of the blocks. The center block is forced at a constant displacement rate between the two side blocks to rate frictional shear. We studied gouge layers ranging from 3-7 mm thick, consisting of smooth glass beads, rough sand particles, or mixtures of both. The experiments are run at room temperature and humidity, and the layers were sheared at rates from 0.1 to 3000 microns per second. Experiments are carried out under a normal stress of 10 MPa, a non-fracture loading regime where sliding friction for smooth spherical particles is measurably lower than for rough angular particles.

Stick-slip instability occurs in gouge that consists of less than 40% angular grains and begins once the coefficient of friction (shear stress divided by normal stress) within the sheared layers reaches a value of 0.35-0.40. Peak friction during sliding is about 0.40-0.45. Each stick-slip event involves a small amount of quasi-static displacement prior to failure, which we refer to as pre-seismic slip. When the shear stress reaches this peak strength, failure occurs, and shear stress drops dynamically. For each experiment we measure the amount of pre-seismic slip that occurs just before failure, and the magnitude fs stress drop that occurs during failure. The amounts of pre-seismic slip and stress drop vary systematically with sliding velocity. Our data show that the amounts of pre-seismic slip and stress drop decrease logarithmically with increasing loading velocity.

Fe-Si COMPLEXES: THEIR IMPORTANCE FOR UNDERSTANDING BANDED IRON FORMATIONS

Ekaterina Bazilevskaya
Advisor: Hiroshi Ohmoto

In the absence of silica-secreting organisms, Precambrian oceans could be much more silica-rich (>150 ppm) than today. If true, this fact can put new constraints on the origin of banded iron formations (BIF). Silica retards precipitation of iron hydroxide and therefore increases the migration ability of iron. The purpose of this research it to study the effect of aqueous silica on precipitation of iron hydroxide over the pH range from 3 to 10 at ambient conditions (T = 25°C, pO_2 = 0.22 atm).

Ferric chloride solution (5 mg/l) was added to sodium silicate solution with various concentrations of silica (0 – 500 mg/l SiO_2). Solution pH was adjusted to a desired value with HCl. Solutions were filtered with a 0.45 nm membrane filter after 24 hours, 7 days, and 30 days. Concentrations of Fe and SiO_2 in the filtrates were measured by ICP-AES.

Results indicate that precipitation of ferric hydroxides and silica is strongly influenced by pH and relative concentrations of Fe and SiO_2 in solution. At SiO_2 concentrations < 110 mg/l (solubility of amorphous silica at pH < 10; T = 25°C), ferric hydroxide precipitates at any pH > 3. Some SiO_2 also co-precipitates with ferric hydroxide probably due to adsorption on ferric hydroxide particles. At SiO_2 concentrations > 110 mg/l, iron hydroxides do not form, and iron rather stays in solution. We suggest the formation of Fe-Si aqueous complexes, which are very stable and thus prevent the precipitation of ferric hydroxides. Also at a given silica concentration, formation of $Fe(OH)_3$ depends on pH.

Therefore, BIF formation could be controlled not only by redox chemistry of iron, but also by the relative abundances of iron and silica in the Precambrian ocean.

CRUSTAL STRUCTURE EVOLUTION IN RESPONSE TO THE PASSAGE OF THE MENDOCINO TRIPLE JUNCTION: A RECEIVER FUNCTION ANALYSIS

Gavin Hayes
Advisor: Kevin Furlong

Deformation in Northern California is driven by the interactions of the Pacific, Gorda and North American plates, which meet at the Mendocino triple junction (MTJ). The complex interactions at this junction have a significant impact on the crustal structure of the North American plate. As the MTJ migrates north, North America is first thickened and then thinned over a distance of a few hundred kilometers, driven by coupling between the subducting Gorda plate and the base of the North American plate. This process causes rapid crustal metamorphism as the triple junction passes, transforming the basal sedimentary facies of the Northern California accretionary margin into crystalline basement.

Superposed on this regional crustal evolution are complexities produced by local interactions between the Pacific and North American plates. In particular small plate fragments captured by (and thus moving with) the Pacific plate, may generate localized crustal thickening and thinning as they migrate subjacent th the western margin of North America. This is seen in the region of the USGS Cahto Peak station, south of the triple junction, where the presence of the Pioneer fragment (captured by the Pacific plate) beneath the North American plate is imaged as a fast seismic anomaly in tomographic studies. Receiver function analysis at Cahto Peak is used to refine and calibrate these tomography seismic images in order to test the conceptual model of plate fragments translating beneath the North American crust. These receiver function results can be compared with existing receiver function analyses at other stations to provide a more regional framework of the crustal evolution of Northern California.

BIOMODULE: A JAVA PROGRAM TO HELP MODEL AND INTERPRET THE STRATIGRAPHIC RECORD

Achim Herrmann
Advisor: Mark Patzkowsky

A combination of a stratigraphic simulation package (STRATA) and an evolutionary-ecological model (BIOSTRAT) can be used to simulate the distribution of species within a sequence stratigraphic framework. BIOMODULE is an extension of this model approach in that it facilitates the visualization and interpretation of those simulations and their input data. Environmental factors (e.g., sea-level changes or sedimentation rates) and ecological factors (different preferred water depth, depth tolerances, abundance) that determine the spatial and temporal distribution of species are easily and quickly investigated. In addition, BIOMODULE can be used to compile the stratigraphic first and last appearances of those species and export them into available graphic correlation software packages (Conop9 and GraphCor). This can be used to test the graphic correlation technique and investigate its accuracy and precision under a range of different conditions (different stratigraphic architectures, sampling densities, etc) since the true correlation of the different sections is already known.

EVOLUTION OF MERAPI VOLCANO, INDONESIA: A CONTRIBUTION USING CSD ANALYSIS

Sabrina Innocenti
Advisor: Tanya Furman

Merapi is an explosive andesitic volcano located in Java, Indonesia; its activity originated 40,000 BP and is related to the subduction of the oceanic Indian plate beneath the Eurasian continent. Merapi's recent eruptive activity is dominated by effusive events involving the construction and collapse of small domes, but its early history was dominated by highly explosive activity as preserved in the tephrostratigraphic record. This change in eruptive style has been accompanied by a fluctuation in silica content and crystallinity of eruptive products. It is imperative to address the full spectrum of eruptive activity in concert with changes in eruptive composition as part of a meaningful hazard assessment for Merapi.

We apply petrographic, geochemical and crystal size distribution (CSD) analyses to samples from both the recent lava dome activity and few very old Merapi products to compare and contrast textural information and geochemical information. Our goal is to determine the intensive parameters attendant to these different eruptive styles, and to explore whether precursors to catastrophic events can be identified within the tephrostratigraphic record. Petrographic studies show evidence of open system behavior represented by multiple crystal generations, suggesting that mafic magma influx is a trigger to small-volume recent eruptive activity as confirmed by geochemical data. Crystallinity, vesciculariy, water content and chemistry will be determined to identify the rheological parameters of the melts and compare them along the stratigraphy. Residence times of magmas in the magma chamber are calculated through plagioclase CSD both for the recent activity and the old activity analyzed.

Through CSD analysis we separate the contribution of syn-eruptive plagioclase crystallization from that of crystal generation within the magma chamber and the conduit. This comparison provides insight into the crystallization history of the eruptive rocks and thus on the magma chamber processes involved.

CRUSTAL STRUCTURE OF NORTH AFRICA, MIDDLE EAST AND SOUTHERN EUROPE

Minoo Kosarian
Advisor: Charles Ammon

Research on North Africa, Middle East and Southern Europe provides an opportunity to work with very diverse crustal structures and tectonic environments. We employ joint inversion of different seismic data sets to estimate crustal structure and thickness of lithosphere. Surface-wave dispersion observations can determine average absolute shear velocity variation with depth; receiver functions provide constraints on the travel-time between velocity contrasts and constrain boundary sharpness. The joint inversion of receiver functions and surface-wave dispersion is a practical tool to estimate lithospheric structure because the combination greatly reduces non-uniqueness of the solution. We examined data recorded by about 20 permanent and temporary three-component broadband seismic stations located in the Middle East, Southern Europe and Northern Africa. We computed over 2100 receiver functions by examining records from 9969 earthquakes in the period of 1990-2002. We adopted the group velocities for both Love and Rayleigh waved from tomographic analyses by the Lawrence Livermore National Laboratory.

In our initial step of analyses, we stacked the receiver functions using the thickness-Vp/Vs ratio estimation procedure of Zhu and Kanamori (2000). This initial analysis provides reasonable constraints on the thickness and Poisson's ration (which trade-off) for each station and helps identify stations on top of complex structures (where simple plane-layered methods will fail). The majority of our crustal thickness estimates are consistent with previous geophysical/seismological work, but there are a few differences. In this presentation, we summarize the Poisson's ration work and present the results of joint surface-wave dispersion and receiver function inversion for some of the stations.

TIME-RESOLVED STRUCTURAL ANALYSIS OF CATION EXCHANGE RATIONS IN BIRNESSITE USING SYNCHROTRON XRD

Christinal Lopano
Advisor: Peter Heaney

Manganese oxides offer some of our most promising resources for the natural and artificial removal of metal toxins in polluted waters. Mn oxides swap cations in and out of their interlayer and intertunnel regions rather than their octahedral sites. The rates of exchange are rapid and are strongly dependent on the hydration state of the mineral. Birnessite ($(Na,Ca,Mn^{2+})\ Mn_7O_{14}\cdot 2.8H_2O$) is a layered Mn-oxide with a 7.2 Å spacing between the Mn octahedral sheets. Since birnessite is an abundant phase in soils, desert varnishes, and ocean nodules, it plays a significant role in soil and groundwater chemistry. Past experiments have demonstrated that Na-buserite (hydrated birnessite) readily exchanges Na+ for a variety of other cations, including K^+, Mg^{2+}, Ca^{2+}, Ba^{2+}, Ni^{2+}, and Sr^{2+}. In light of its high cation exchange capacity, birnessite is industrially important for used in ion and molecular sieves and cathodic material, and environmentally important for possible incorporation of heavy metal pollutants. In addition, birnessite serves as a precursor in the synthesis of todorokite, which has a 3x3 tunnel structure and is used as an octahedral sieve.

We monitored cation-exchange reactions in birnessite by time-resolved X-ray powder diffraction through a simple flow-through cell at the National Synchrotron Light Source. The flow-through cell was developed by Lee and Parise at SUNY-Stony Brook, and this work represents its first application to Mn oxides. A series of synthetic Na-birnessite samples were saturated with chloride solutions containing dissolved K^+, Mg^{2+}, and Ba^{2+}, ranging from 0.1M to 0.001M. These cations were selected in preliminary experiments because their crystal structures are well documented. Powder X-ray diffraction patterns were collected every ~ 3 minutes as solution flowed through the cell. The synchrotron experiments revealed that complete cation exchange occurs within 3 hours, and significant modifications of the arrangements of the interlayer cations and water molecules accompany the exchange. Specifically, the replacement of Na by Mg resulted in the continuous growth of a discrete buserite-like phase with a 10 Å layer spacing, while replacement of Na by K and Ba retained the 7 Å spacing. K replacement of Na resulted in gradually decreasing peak intensity and peak merging. The Ba exchange yielded an abrupt decrease in diffraction intensities followed by a more gradual lattice change over the last 2 hours. Rietveld analysis led to the first determination of the structure of Ba-birnessite and K-birnessite in a triclinic space group.

GROUND TRUTH FROM REGIONAL SEISMIC NETWORKS IN NORTHEASTERN AFRICA

Yongcheol Park
Advisor: Andrew Nyblade

The objective of this work is to develop a catalog of reference events (ground truth) in the northeast African Area. The ground truth catalog is assembled by determining origin time, focal mechanism and hypocenters with accuracies of 10 km or better (GT 10), using these events to construct regional travel time correlation surfaces, and using travel time correction surfaces to obtain origin times and epicenter for numerous other events.

To obtain focal mechanisms, I use a grid search algorithm to find acceptable solutions based on P, SV and SH polarities and amplitude ratios (SV/P, SH/P and SV/SH). Focal depths are determined by waveform modeling using wavenumber integration and by comparing observed seismograms with synthetic seismograms for varying source depths. Epicentral locations are finally determined by fixing the source depth and using P and S travel times.

I have determined source parameters (focal mechanism, magnitude, origin time, epicenter and depth) of 3 events in Ethiopia recorded by the Ethiopian Broadband Seismic Experiment. The results are summarized in the table below. These are preliminary results, and I will add more earthquakes and improve locations (including source depth) by using data from the closest stations. To do this, observed and calculated incidence angle and ray parameter obtained from one or two stations will be compared to constrain source depth, epicentral distance and back azimuth.

Table 1. Hypocenter parameters and focal mechanism

Event no.	Latitude	Longitude	Data Origin Time mm/dd/yy	Depth (km)	Focal Mechanism Strike	Dip	Rake
1	9.32°N	40.79°E	05/16/00 20:47:51.94	4	102.44	25.92	25.06
2	6.87°N	37.97°E	03/11/01 00:42:42.09	5	210.00	45.00	90.00
3	6.87°N	37.96°E	03/12/01 16:40:07.30	10	108.29	38.50	21.80

NEAR-REAL SOURCE PARAMETER ESTIMATION OF SMALL-TO-MODERATE SIZED EARTHQUAKES (MW < 5.5) USING REGIONAL WAVEFORM DATA

Winchelle Sevilla
Advisor: Charles Ammon, Harley Benz

The purpose of this study is to construct and test earth structure models that can be used for near-real time source parameter estimation of small to moderate-sized (Mw<5.5) North American earthquakes using regional data. I used three different velocity models, which I called A-model, H-model, and C-model, to represent the structure beneath the conterminous U.S. At the present, the National Earthquake Information Center (NEIC) has the capability to do near real-time source parameter estimation of earthquakes with magnitude (Mw) 5.5 and larger, where they use teleseismic data for source parameter estimation. I use seismograms recorded at regional distances because teleseismic stations seldom produce well-recorded data for the magnitude range considered here.

Four moderate-sized earthquakes were chosen to approximately sample the conterminous U.S. To estimate the moment tensor, I modeled the complete displacement waveforms in the period range of 50 to 20 sec and recorded at stations between 1 and 15 degrees using Kennett's (1983) reflection-matrix method as implemented by George Randall. A least-squares time domain inversion of the complete waveforms is performed from 5 to 30 km depth at 2.5 km intervals to estimate the optimal moment tensor solution of four earthquakes.

Results (e.g. faulting parameters, focal depth, moment magnitude, focal mechanisms) from the tests show that each solution agrees well with the findings of other workers who modeled earthquakes. This work is still at its early stage but the estimated source parameters using the A-model and perhaps the H-model look feasible for near real time source parameter estimation. Further testing of the A-model will be the future thrust of this work to assess the extent by which the said model can give valid estimates of source parameters for the moderate-size earthquakes of the conterminous U.S.

CRUSTAL STRUCTURE BENEATH THE EAST AFRICAN RIFT SYSTEM

Mulugeta Tuji and Jordi Julia
Advisor: Andrew Nyblade

H-Kappa (Moho depth (H) and Vp/Vs ratio (Kappa)) analysis technique is applied to study crustal structure beneath eastern Africa, especially beneath and adjacent to the East African Rift Valley. HK analysis is a direct search method for Moho depth and Vp/Vs ratio through a predetermined parameter space. The technique is based on the idea that a stack of the weighted sum of receiver functions amplitudes at the arrival times for the Ps converted and the two first multiples in the P wave coda will attain a maximum value when there is coherent stacking. Moho depth and Poisson's ratio have also been determined using simple stacks of the receiver functions.

Seismic data have been recorded by an array of 36 temporary seismic stations in Ethiopia and Kenya from 2000 to 2002. For the study at hand, we are making use of these data along with data from permanent stations in the region. These include ATD, FURI, KMBO, MBAR, NAI.

The two methods for analyzing receiver functions yield consistent results. Moho depth varies between 23km in the rift to 44km in the highland areas away from the rifts. The range of the poisson's ratio observed for the crust beneath most of the stations is 0.23 to 0.28. A high value of 0.24 is observed for the Afar.

A BROADBAND SEISMOLOGICAL INVESTIGATION OF THE UPPER MANTLE STRUCTURE BENEATH THE TRANS ANTARCTIC MOUNTAINS AND EAST ANTARCTIC REGION

Timothy Watson
Advisor: Andrew Nyblade

The Trans Antarctic Mountains (TAM), among the world's foremost mountain ranges, consist of gently tilted fault blocks resulting from vertical crustal movement during the Cenozoic. Paralleling much of the West Antarctic Rift System, the TAM are considered by many to be a classic example of the rift flank uplift, however evidence supporting a clear uplift mechanism has yet to be provided. Additionally, the adjacent East Antarctic Craton exhibits anomalously high elevation for a cratonic block when corrected for glacial loading. To investigate these two unique tectonic features the broadband seismic experiment TAMSEIS (Tran Antarctic Seismic Experiement)) was conducted, utilizing 44 broadband seismometers spread across three arrays, to record seismic waves passing through the upper mantle and crust beneath portions of the TAM and East Antarctic craton. We believe that the thermal state of the upper mantle TAM and East Antarctic craton. We believe that the thermal state of the upper mantle beneath these regions will provide the information necessary to discriminate between the competing uplift models. To investigate the temperature variations of the upper mantle, I intend to perform body-wave tomography using P and S wave travel time delays obtained from the multichannel cross-correlation method of VanDecar and Crosson (1991).

MICROBIAL INFLUENCES ON TRACE METAL CYCLING IN A MEROMICTIC LAKE, FAYETTEVILLE GREEN LAKE, NY

Aubrey Zerkle
Advisors: Crhistopher House and Lee Kump

Microorganisms can exist in aquatic environments at very high cell densities of up to 10^{11} cells/L, and can accumulate significant quantities of trace metals. Bacteria actively take up bioactive trace metals, including Fe, Zn, Mn, Co, Ni, Cu, and Mo, which function as catalytic centers in metalloproteins and metal-activated enzymes involved in virtually all cellular functions. In addition bacteria may catalyze the release of trace metals from inorganic substrates by processes such as the reduction of iron and manganese oxides, suggesting the trace metal distribution within a natural environment dominated by microbial processes may be influenced by microbial ecology. Fayetteville Green Lake (FGL), NY, is a permanently stratifies meromictic lake that has a well-oxygenated surface water mass (mixolimnion) overlying a relativity stagnant, anoxic deep water mass (monimolimnion). A chemocline separated the water masses at around 20m depth, where oxygen concentrations decrease and sulfate and methane concentrations increase. In addition, previous studies have indicated that trace metals such as V, Cr., Co, Mn, and Fe reach elevated concentration at the chemocline. Using fluorescent in situ hybridization (FISH) of FGL samples from depths of up to 40m with bacterial and archaeal probes, we have shown that fluctuating redox conditions within the FGL water column correlate with significant variations in the composition and distribution of microbial populations with depth. The mixolimnion is dominated by Eubacteria, with increasing concentration of Archaea in the lower anoxic zone. Increases in microbial cell densities coincide with increase in trace metals at the chemocline, suggesting microbial activity may be catalyzing trace metal release at this boundary. 16S rRNA PCR cloning techniques are currently being used to identify dominant microbial populations at various levels with the FGL water column. Future studies will focus on the potential for these dominant microorganisms to influence trace metal cycling and bioavailability in the FGL water column.